Molecular Cell, Vol. 11, 853–864, April, 2003, Copyright ©2003 by Cell Press

Removal of a Single Pore Subcomplex Results in Vertebrate Nuclei Devoid of Nuclear Pores

Amnon Harel,[1,6] Arturo V. Orjalo,[1,6] Thomas Vincent,[1,3] Aurelie Lachish-Zalait,[2] Sanjay Vasu,[1,4] Sundeep Shah,[1,5] Ella Zimmerman,[2] Michael Elbaum,[2] and Douglass J. Forbes[1,*]

[1]Section of Cell and Developmental Biology
Division of Biology 0347
University of California, San Diego
La Jolla, California 92093

[2]Department of Materials and Interfaces
Weizmann Institute of Science
Rehovot 76100
Israel

[3]Isis Pharmaceuticals

[4]Quorex Pharmaceuticals
Carlsbad, California 92008

[5]Aurora Biosciences
San Diego, California 92121

Summary

The vertebrate nuclear pore complex, 30 times the size of a ribosome, assembles from a library of soluble subunits and two membrane proteins. Using immunodepletion of *Xenopus* nuclear reconstitution extracts, it has previously been possible to assemble nuclei lacking pore subunits tied to protein import, export, or mRNA export. However, these altered pores all still possessed the bulk of pore structure. Here, we immunodeplete a single subunit, the Nup107-160 complex, using antibodies to Nup85 and Nup133, two of its components. The resulting reconstituted nuclei are severely defective for NLS import and DNA replication. Strikingly, they show a profound defect for every tested nucleoporin. Even the integral membrane proteins POM121 and gp210 are absent or unorganized. Scanning electron microscopy reveals pore-free nuclei, while addback of the Nup107-160 complex restores functional pores. We conclude that the Nup107-160 complex is a pivotal determinant for vertebrate nuclear pore complex assembly.

Introduction

The nuclear pore complex (NPC) is a significant barrier to proteins requiring import, and mRNAs, tRNAs, and ribosomes requiring export. For much of nucleocytoplasmic traffic, receptors of the importin-β family ferry cargo through the NPC. Distinct from this, mRNAs also employ other proteins for their export (Gorlich and Kutay, 1999; Conti and Izaurralde, 2001; Feldherr et al., 2001; Weis, 2002; Shamsher et al., 2002). Traffic through the NPC is globally regulated by the small GTPase Ran (Sazer and Dasso, 2000; Damelin and Silver, 2000; Kalab et al., 2002; Macara, 2002; Schwoebel et al., 2002). Viruses often opportunistically alter the rules of nuclear trafficking in order to import their genomes or inhibit cellular mRNA export (Cullen, 2001; Conti and Izaurralde, 2001).

The vertebrate NPC contains multiple structural domains (Figure 1A). These include cytoplasmic filaments, thin nuclear and cytoplasmic rings, a scaffold of eight large spokes, a central transporter region, and a "basket" of nuclear filaments (Hinshaw et al., 1992; Yang et al., 1998; Goldberg et al., 1997; Rout et al., 2000). The crucial central transporter region contains nucleoporins with abundant phenylalanine-glycine (FG) repeats. In vertebrates, these are the Nup62/58/54/45 proteins (Figure 1A, dark green) (Vasu et al., 2001). Transport receptors enter the central region through affinity for these FG repeats, while other proteins are excluded. The precise mechanism of translocation remains a source of debate (Rout et al., 2000; Ribbeck and Gorlich, 2002; Siebrasse and Peters, 2002).

Given the importance of the nuclear pore complex, an understanding of its molecular structure has lagged significantly. This results from the massive size of the NPC (120 million daltons in vertebrates; 60 MDa in yeast), the complexity of its traffic, and the fact that its full complement of ~30 proteins was only recently revealed (Reichelt et al., 1990; Rout et al., 2000; Miller and Forbes, 2000; Cronshaw et al., 2002). Yeast NPC proteins differ substantially from those of vertebrates (Vasu and Forbes, 2001). However, in both, only a few components are integral membrane proteins, while the majority are recruited from the cytoplasm in dozens of copies as small preformed subunits (Matsuoka et al., 1999). The contacts between the subunits, their location in the NPC, and the mechanism of NPC assembly remain, to a large extent, speculative.

Recently, a new vertebrate NPC subcomplex was discovered by virtue of its interaction with Nup153 and Nup98 (Vasu et al., 2001), the two most critical nucleoporins for mRNA export (see Bastos et al., 1996; Powers et al., 1997; Ullman et al., 1999; Dimaano et al., 2001; Griffis et al., 2002; and references therein). This new subcomplex minimally was found to contain five proteins: Nup160, Nup133, Nup107, Nup96, and sec13 (Belgareh et al., 2001; Vasu et al. 2001; see also Fontoura et al., 1999). Previous names for the complex are combined here for clarity into a compound name, the Nup107-160 complex. This complex localizes to both sides of the NPC by electron microscopy (Belgareh et al., 2001). Domains of two of the proteins, Nup160 and Nup133, have strong dominant-negative effects on mRNA export in vivo (Vasu et al., 2001). Surprisingly, a fraction of the Nup107-160 complex migrates to the kinetochores during mitosis, implying that the complex has a separate mitotic role (Belgareh et al., 2001; Lyman and Gerace, 2001).

Members of the vertebrate Nup107-160 complex have homology to the yeast Nup84 complex (Nup84p, Nup85p, Nup120p, Nup145Cp, sec13, and seh1). Yeast mutants show mRNA accumulation and NPC clustering (Doye et al., 1994; Aitchison et al., 1995; Goldstein et

*Correspondence: dforbes@ucsd.edu

[6]These authors contributed equally to this work.

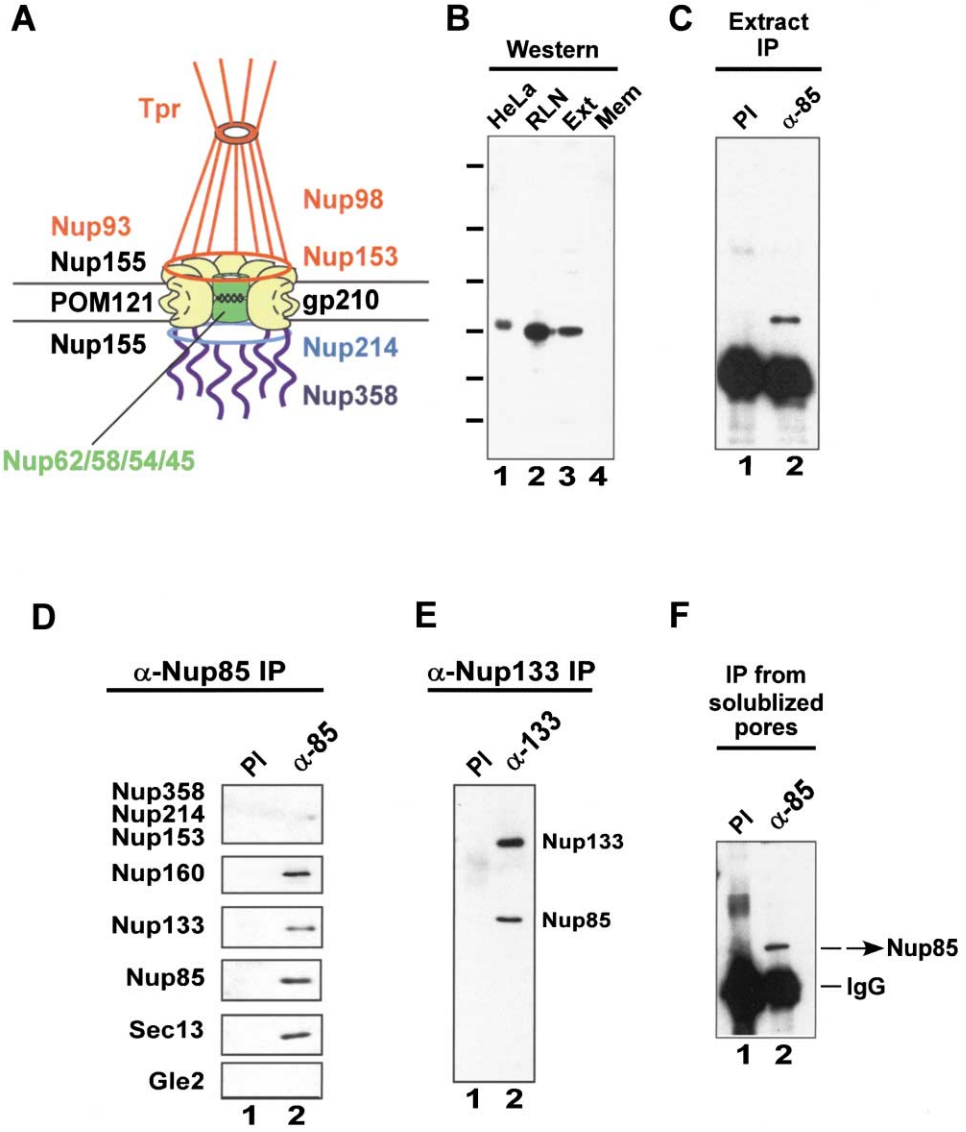

Figure 1. Metazoan Nup85, a New Component of the Nup107-160 Complex

(A) A model of vertebrate NPC structure, showing the cytoplasmic filaments (dark blue), cytoplasmic ring (blue), central scaffold spokes (yellow-green), central transporter (dark green), and nuclear ring and nuclear pore basket (red). The approximate location of a subset of nucleoporins is shown.

(B) Anti-mouse Nup85 antibody recognizes a single ~70 kDa protein in HeLa cell extract (lane 1, 1 μl, 10 μg total protein), rat liver nuclei (lane 2, 1 μl; ~12,000 nuclei), and in *Xenopus* egg cytosol (lane 3, Ext, 0.1 μl) but not membranes (lane 4, 0.1 μl). Markers are 200, 120, 90, 68, 53, and 36 kDa.

(C) Immunoprecipitation from *Xenopus* egg cytosol using anti-mNup85 (lane 2) and preimmune sera (lane 1). The blot was probed with anti-mNup85.

(D) Immunoprecipitation from HeLa cell extracts using anti-mNup85 (lane 2) and preimmune sera (lane 1). The blot was cut horizontally and probed with mAb414 (to detect Nup358, Nup214, and Nup153) and individual antisera to Nup160, Nup 133, Nup85, sec13, and Gle2. The FG nucleoporins and Gle2 were absent from these immunoprecipitates (lane 2), as were Nup62, Nup93, Nup98, Nup155, and Nup205 (data not shown).

(E) Immunoprecipitation from HeLa cell extracts using anti-hNup133 (lane 2) and preimmune sera (lane 1); the blot was probed with anti-hNup133 and anti-mNup85 antisera.

(F) Nup85 is present in assembled pores. Annulate lamellae were assembled, and the pores were purified (Miller and Forbes, 2000) and partially solubilized before immunoprecipitation with anti-mNup85. Nup85 was immunoprecipitated from purified pores by anti-Nup85 (lane 2).

al., 1996; Li et al., 1995; Siniossoglou et al., 1996, 2000; Lutzmann et al., 2002, and references therein). Although no single Nup84 complex gene is essential, mutations in any two cause synthetic lethality. The yeast Nup84 complex forms a Y-shaped structure, and addition of *S.c.* Nup133 lengthens this Y to ~40 nm (Siniossoglou et al., 2000; Lutzmann et al., 2002). The complex theoretically could form part of the basket filaments, a subunit

of the rings, a portion of the spokes, or some other structure of the yeast NPC.

In vertebrates, nuclear reconstitution has proven to be a powerful tool for assigning function to nucleoporins. Nuclei reconstituted in vitro from *Xenopus* egg extracts contain double nuclear membranes and nuclear pore complexes and show robust import, DNA replication, and pol III transcription (Forbes et al., 1983; Lohka and Masui, 1983; Blow and Laskey, 1986; Newport, 1987; Ullman and Forbes, 1995; Zhang and Clarke, 2000). When egg extracts are immunodepleted of the central transporter components, Nup62/58/54/45, the resulting nuclei are defective for import (Finlay et al., 1991). In contrast, when nuclei are reconstituted without the cytoplasmic ring protein Nup214 or the basket protein Nup98, both known to play a role in export, the nuclei have no defect in import (Powers et al., 1995; Grandi et al., 1997; Walther et al., 2002). Nuclei reconstituted without Nup153 are found to lack the basket-associated proteins Nup98, Nup93, and Tpr, while nuclei missing Nup358 lack cytoplasmic filaments (Walther et al., 2001, 2002). Thus, in each of these cases, removal of a nucleoporin and its immediate neighbors chips away at NPC structure but does not affect it at its central core.

In search of essential building blocks of the vertebrate nuclear pore, we examined the Nup107-160 complex. Using immunodepletion and nuclear reconstitution, we have unexpectedly identified the biochemical equivalent of a null mutant for the vertebrate nuclear pore. Absence of the Nup107-160 complex gives rise to nuclei with strikingly severe defects in NPC structure and assembly.

Results

Antibodies to Vertebrate Nup85, a New Component of the Nup107-160 Complex

One arm of the yeast Y-shaped Nup84 complex is composed of Nup85 and seh1 (Siniossoglou et al., 2000; Lutzmann et al., 2002). The related vertebrate Nup107-160 complex was puzzling in that there was no readily apparent Nup85 candidate, either by simple BLAST searches or silver staining (Vasu et al., 2001; Belgareh et al., 2001). When a more stringent PSI-BLAST search was done, however, we identified mouse ESTs which could be pieced together to encode a putative ORF of 656 aa. A PSI-BLAST search with this ORF sequence revealed relatives from humans to *S. pombe* ranging in size from 598–733 aa, as well as the *S. cerevisiae* Nup85 (744 aa).

This mouse ORF was cloned, expressed as protein, and antibody raised. The antibody recognized a single ~70 kDa band in humans, rats, and *Xenopus* (Figures 1B and 1C). It further coimmunoprecipitated Nup160, Nup133, and sec13, three known members of the vertebrate Nup107-160 complex (Figure 1D), but not other nucleoporins. Anti-Nup133 antibody conversely coimmunoprecipitated the 70 kDa protein (Figure 1E). Pull-downs with the Nup153 beads originally used to identify the Nup107-160 complex in *Xenopus* (Vasu et al., 2001) were also found to contain the 70 kDa protein (data not shown). Most tellingly, the ~70 kDa protein was present in purified *Xenopus* pores (Figure 1F) (Miller and Forbes, 2000).

Immunofluorescence with the anti-70 kDa antibody produced a punctate nuclear rim stain (Figure 2A), while transfection of a myc-tagged version showed incorporation into NPCs (Figure 2B). We conclude that the ~70 kDa mouse protein and its relatives are indeed vertebrate Nup85. The *Xenopus* Nup85 protein sequence (data not shown) has ~55% identity to mouse Nup85, explaining its strong crossreactivity with the anti-mouse Nup85 antibody (Figures 1B, 1C, and 1F). Near the end of our study, a proteomic analysis of NPC proteins solubilized from rat nuclear envelopes observed a rat Nup85 homolog and termed the human relative hNup75 (Cronshaw et al., 2002). Our data indicate that we have identified Nup85 homologs from *S. pombe, Drosophila, C. elegans*, rice, *Arabidopsis*, and humans, with sizes ranging from 68 to 85 kDa (see Experimental Procedures). For clarity and consistency with yeast, we collectively term the proteins Nup85. Metazoan Nup85 is quite dissimilar from yeast Nup85, having only 13%–14% identity. Structurally, human Nup85 is α-helical (GOR4 Program) and contains no obvious conserved domains or FG repeats.

Nup85 Is Present at the Kinetochores of Mitotic Chromosomes

At interphase, the Nup107-160 complex plays a role in mRNA export (Vasu et al., 2001). During mitosis, however, a fraction of the complex moves to the kinetochores (Belgareh et al., 2001). We found Nup85 to show the same strong mitotic association with kinetochores (Figures 2C and 2D). Thus, Nup85 is concluded to be available for participation with the Nup107-160 complex in its as yet unknown role at the mitotic kinetochores.

Anti-Nup85-Depleted Nuclei Are Deficient in NPC Number and Import

Recent advances in metazoan cells have used transfection of small double-stranded interfering RNAs (RNAi) to target the destruction of specific mRNAs (Elbashir et al., 2001). We initially attempted to knock out Nup85 in HeLa cells using RNAi. A large but incomplete reduction in the Nup85 nuclear rim stain was indeed observed (Figure 2E). Interestingly, the FG nucleoporins which map throughout the length of the NPC were also greatly reduced (Figure 2F). This suggested that the removal of Nup85 might cause extensive defects in the NPC. These results, while provocative, represented only a partial knockout (see also Boehmer et al., 2003). The desire for a more complete knockout led us to attack the role of Nup85 at the level of pore complex assembly.

Nuclear reconstitution can be accomplished in vitro by combining chromatin with the membrane and cytosol fractions of a *Xenopus* egg lysate. Antibody to Nup85 was used here to immunodeplete Nup85 and its associated proteins from the cytosol, while preimmune IgG was used for mock-depletion. The great majority of Nup85 was removed by immunodepletion (Figure 3A, lane 2). Strikingly, Nup133 and Nup160 were also largely removed (Figure 3C, lane 2). In addition, sec13 was partially depleted (Figure 3C), consistent with its presence both in the Nup107-160 complex (depleted) and a separate vesicular trafficking complex (not depleted) (Shay-

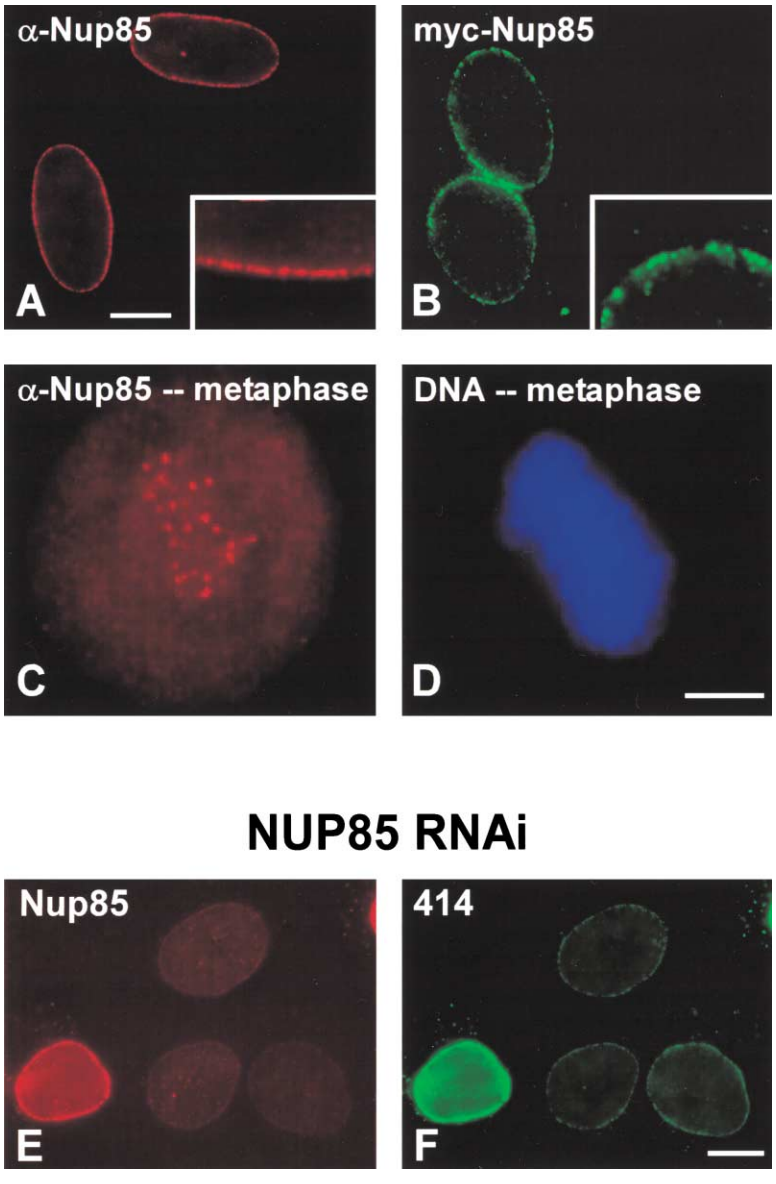

Figure 2. Nup85 Is Present in NPCs and on Mitotic Kinetochores

(A) Immunofluorescence with anti-mNup85 antibody on HeLa cells; the inset shows a magnified portion, revealing the punctate nuclear rim.

(B) Transfection of myc-tagged mNup85 into HeLa cells and immunofluorescence with anti-myc antibodies. Mouse Nup85 localizes to human NPCs. The inset shows a magnified portion of the nuclear rim and individual NPCs.

(C and D) A mitotic cell from the experiment in (A) is shown stained with anti-mNup85 (C) and the DNA dye DAPI (D). A fraction of Nup85 localizes to the kinetochores.

(E and F) RNAi was performed on HeLa cells using dsNup85 oligomers. At 72 hr, RNAi greatly reduced the amount of Nup85 present in the NPCs, as assessed using anti-Nup85 antibodies (Nup85), and prevented the majority of FG nucleoporins from associating with nuclear NPCs, as assessed with mAb414 antibody (414). The scale bar represents 10 μm in (A) and (B) and (E) and (F), 5 μm in (C) and (D), and ~2.7 μm in the insets for (A) and (B).

witz et al., 1995; Vasu et al., 2001; Cronshaw et al., 2002). The FG-nucleoporins Nup358, Nup214, Nup153, and Nup62 were undepleted (Figure 3B, lane 2), as were multiple other nuclear proteins, including PCNA, importin α and β, transportin, Nup93, Nup155, and Nup205 (data not shown). Nup98 and Tpr showed a limited depletion (Figure 3C, lane 2; see also below). Overall, we conclude that anti-Nup85 depletion removes the majority of the Nup107-160 complex, as determined by the simultaneous decrease in Nup85, Nup133, and Nup160.

To assemble nuclei lacking the Nup107-160 complex, anti-Nup85-depleted cytosol (Δ85) was combined with chromatin and membrane vesicles and incubated for 60 min to allow for nuclear growth. Fluorescently labeled nuclear import substrate (TRITC-NLS-HSA) was then added. The Δ85-depleted nuclei proved to be quite small and almost completely defective for classical NLS import (Figure 3D). Monoclonal mAb414, which recognizes FG-containing nucleoporins, gave a bright punctate nuclear rim on mock-depleted nuclei (Figures 4A and 4B, MOCK), but showed a dramatically reduced stain on Δ85-depleted nuclei, with very few visible NPCs (Figures 4A and 4B, Δ85). Moreover, individual antibodies to the basket nucleoporin Nup153 or the cytoplasmic ring/filament protein Nup214 failed to stain Δ85-depleted nuclei (Figure 4C). Thus, anti-Nup85 removal of the Nup107-160 complex, although not complete, resulted in nuclei which not only showed a large decrease in NPC number, but lacked basket and cytoplasmic ring/filament proteins.

Complete Immunodepletion of the Nup107-160 Complex Yields Nuclei Devoid of NPCs

In the anti-Nup85 depletion above a small amount of Nup85, Nup133, and potentially other complex members remained (Figure 3C). To attempt to more completely deplete the complex, an antibody to human Nup133

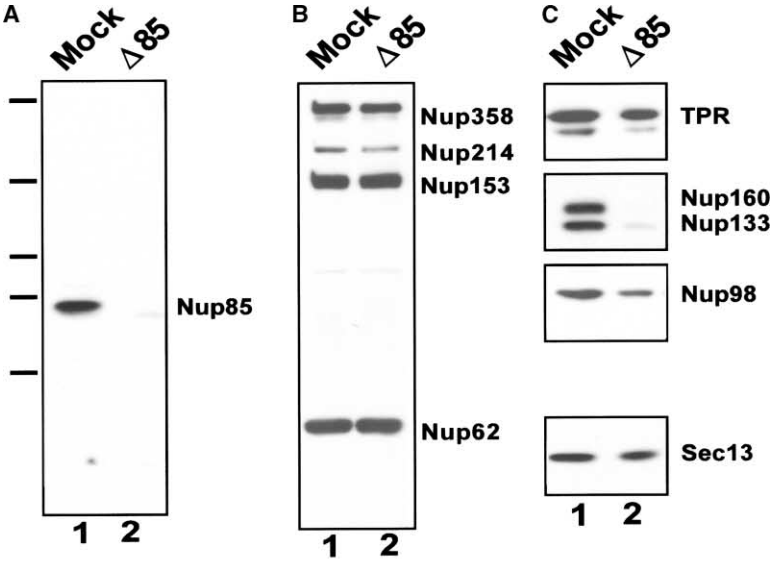

Figure 3. Nup85-Depleted Nuclei Are Small and Deficient for Classical NLS Import

(A) Anti-mNup85 antibodies (lane 2), but not preimmune antibodies (lane 1), immunodeplete the majority of Nup85 from *Xenopus* egg cytosol.

(B) Nup358, Nup214, Nup153, and Nup62 were not immunodepleted by anti-Nup85 (lane 2) antibodies as demonstrated by immunoblotting with mAb414 antibodies.

(C) Immunodepletion of Nup85 largely codepleted Nup160 and Nup133. Sec13 was ~50% depleted and Tpr slightly depleted. For this, blots of mock- (lane 1) and Nup85-depleted (lane 2) cytosol were cut horizontally and probed with individual antibodies to the above and to Nup98.

(D) Nuclei formed in mock- (MOCK) and anti-Nup85-depleted (Δ85) extracts were tested for import by adding TRITC-NLS-HSA transport substrate 60 min after nuclear assembly was initiated and by incubating an additional 60 min. There was no effective import in Δ85 nuclei. The bar represents 10 μm.

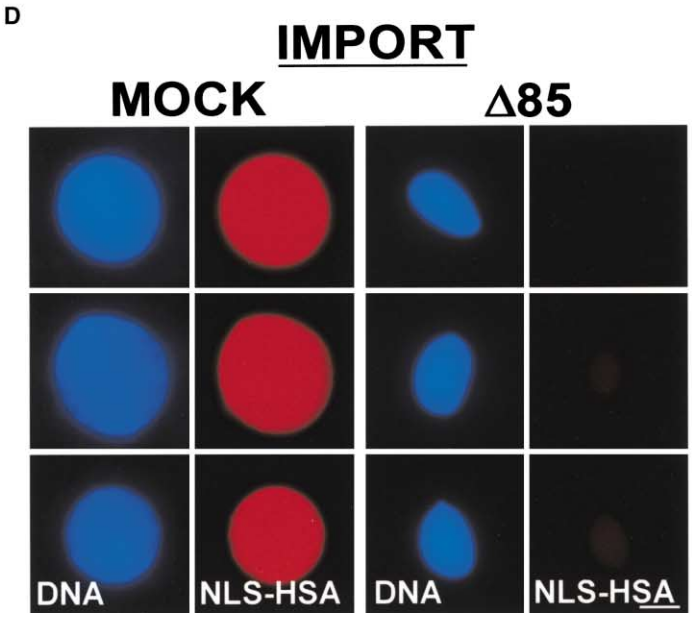

which immunoprecipitates *Xenopus* Nup133 was used. Following anti-hNup133 immunodepletion, all detectable Nup133, Nup160, and Nup85 were removed (Figure 5A, lanes 2 and 4). Sec13 was ~50%–70% depleted (Figure 5C, lane 2), consistent with its presence in two complexes. Other nucleoporins, such as Nup93 (Figure 5A), Nup358, Nup214, Nup153, Nup62 (Figure 5B), Nup155 and Tpr (Figure 5C), remained undepleted. The only exception was Nup98, which was significantly reduced (Figure 5C, lane 2) (see Discussion). In multiple experiments, Δ133 depletion removed all detectable Nup107-160 complex.

The resulting mock- and Δ133-depleted extracts were used for nuclear assembly. While the mock-depleted nuclei were large and capable of robust import, the Δ133-depleted nuclei were extremely small and failed to import (Figure 6A). They did, however, exclude fluorescent dextran, demonstrating the presence of intact nuclear membranes (150 kDa FITC dextran; data not shown). DNA replication in the Δ133-depleted nuclei was acutely compromised (Figure 5F).

Strikingly, Δ133 nuclei had no visible nuclear pore complexes when probed by immunofluorescence using antibodies to the FG nucleoporins (mAb414; Figure 6B), to Nup155 which is normally present on both sides of the NPC (Figure 6C), to Nup93 (Figure 6C), or to the basket nucleoporin Nup153 (data not shown). Indeed, the immunofluorescence defects were more severe than

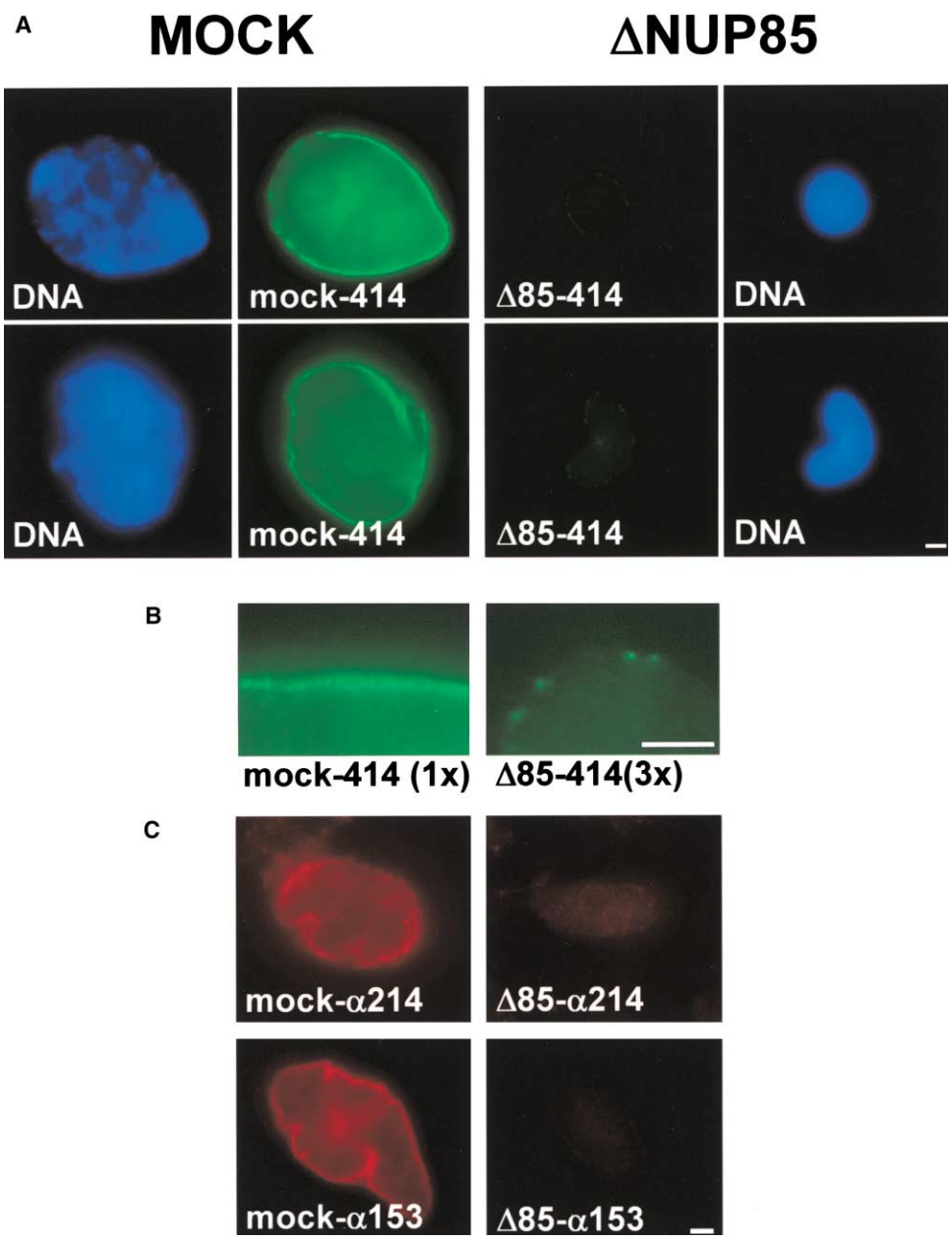

Figure 4. Nuclei Formed in Nup85-Depleted Extract Are Impaired in NPC Assembly

(A) Nuclei reconstituted in mock-depleted (MOCK) and anti-Nup85-depleted cytosol (Δ85) for 90 min were fixed and stained 60 min with directly labeled Oregon green-mAb414 antibody (mock-414 or Δ85-414). Δ85-depleted nuclei were small and stained poorly with the mAb414, indicating a defect in NPC assembly.

(B) Higher magnification views of (A), showing portions of the nuclear rims of mock-depleted (mock-414, 1X exposure) and Δ85-depleted (Δ85-414, 3X exposure) nuclei. A longer exposure was required to see the more lightly staining pores of Δ85-depleted nuclei.

(C) Mock-depleted nuclei and Δ85-depleted nuclei were assembled 60 min, fixed, and subjected to immunofluorescence with anti-Nup214 (α214) and anti-Nup153 (α153) antibodies and TRITC-labeled secondary antibody. The Nup85-depleted nuclei lack Nup214 and Nup153. The bar represents 3 μm in (A) through (C).

those seen in Δ85 depleted nuclei, in that there were no NPCs stained (Figures 6B and 6C).

When small amounts of highly purified Nup107-160 complex (Figures 5D and 5E) were added back to the Δ133-depleted extract at t = 0, this complex was able to restore import function in the resulting nuclei (Figure 6A, addback). Moreover, abundant NPCs that stained with anti-FG antibody were now present (Figure 6B, addback). These last results indicate that the defects are specifically due to the absence of the Nup107-160 complex.

Defects in Integral Membrane Pore Protein Localization

We next tested for presence of the integral membrane proteins of the NPC, POM121 and gp210, in the depleted nuclei (Hallberg et al., 1993; Greber et al., 1990). POM121

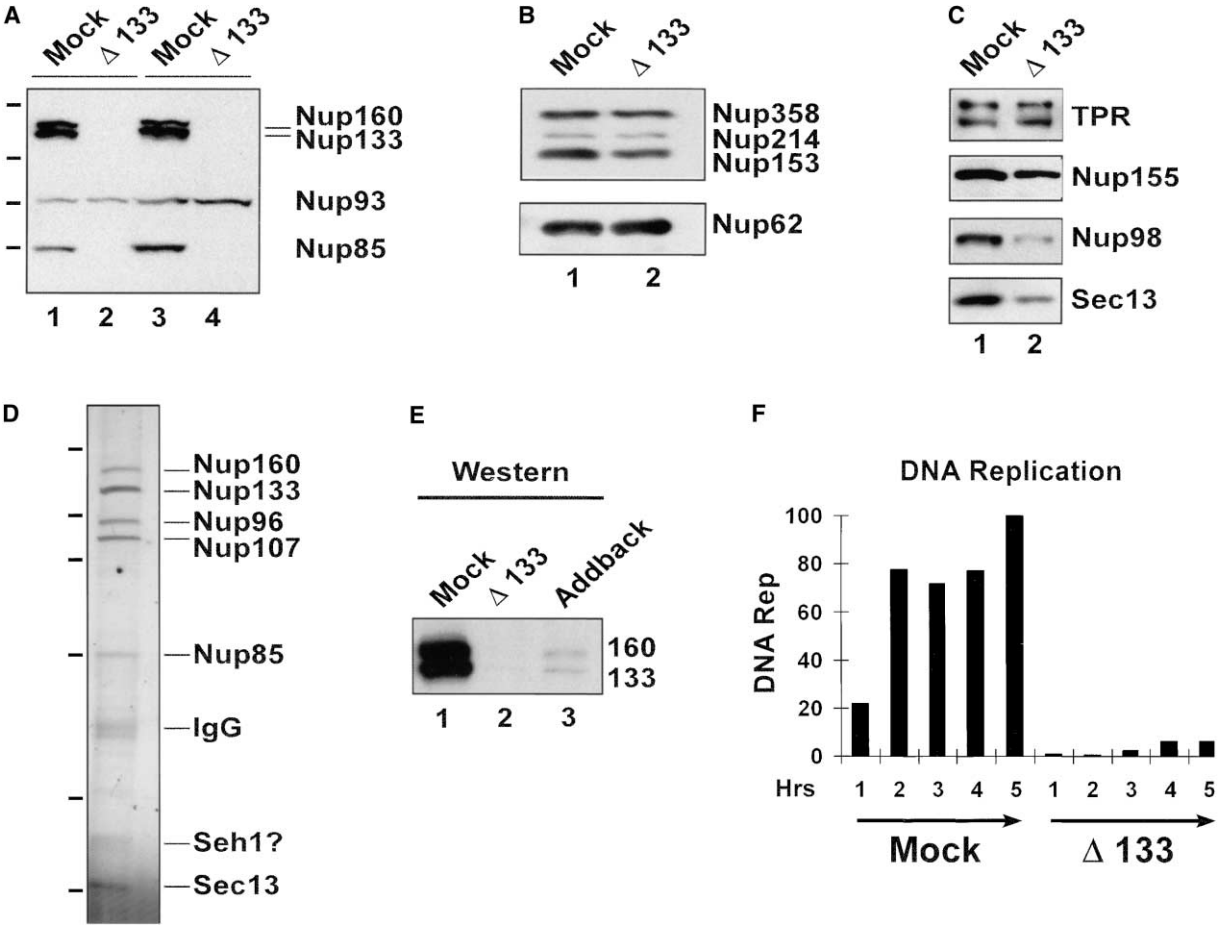

Figure 5. Immunodepletion and Isolation of the Nup107-160 Complex Using Nup133 Antibodies

(A) Anti-hNup133 immunodepletion of *Xenopus* cytosol removes all visible Nup133, Nup160, and Nup85 (mock-depleted, lanes 1 and 3; Δ133-depleted, lanes 2 and 4). A blot of the fractions (lanes 1 and 2, 0.5 μl; lanes 3 and 4, 1 μl) was cut horizontally and probed separately with anti-Nup160 and anti-Nup133 (top), anti-Nup93 (middle), and anti-Nup85 (bottom) antisera.

(B) The cytosolic fractions in (A) were immunoblotted with mAb414, showing that Nup358, Nup214, Nup153, and Nup62 are not significantly immunodepleted.

(C) The mock- and Δ133-depleted *Xenopus* egg cytosols were immunoblotted with anti-Tpr, Nup155, Nup98, and sec13 antibodies. Diminution of Nup98 and sec13 was observed.

(D) Silver-stained SDS-PAGE analysis of immunopurified Nup107-160 complex. The identities of Nup160, Nup133, Nup85, and sec13 were verified by immunoblot analysis. Nup96 and Nup107 were ascertained from protein sequencing in previous work (Vasu et al., 2001). Residual amounts of IgG and ovalbumin are present. The position of a putative Seh1 homolog (Band 31, Cronshaw et al., 2002) is also shown.

(E) To compare the relative amount of the Nup107-160 complex added back to rescue Δ133 cytosol, samples (0.2 μl) of the nuclear reconstitution reactions shown in Figure 6A (mock, Δ133, and addback) were probed with anti-Nup160 and anti-Nup133 antisera.

(F) Replication in Δ133-depleted nuclei is severely inhibited compared to that in mock-depleted nuclei. Replication (%) was normalized to 100% of that seen in mock-depleted nuclei at 5 hr; 1, 2, 3, 4, and 5 hr time points are shown.

was probed with directly labeled Oregon-green anti-POM121 antibody in parallel with red TAMRA-labeled mAb414. Anti-POM121 antibody gave a strong punctate nuclear rim in mock-depleted nuclei, but showed only a faint hazy stain of Δ133 nuclei (green, Figure 6D, top four panels).

Texas red-labeled anti-gp210 antibody also gave a strong punctate nuclear rim on mock-depleted nuclei, but only a faint diffuse stain of Δ133 nuclei (red, Figure 6D, bottom four panels). In both experiments, anti-FG antibody (mAb414) showed no staining of the complex-depleted nuclei (Figure 6D). We conclude that nuclei lacking the Nup107-160 complex are either unable to recruit the integral membrane pore proteins to the newly formed nuclei or, if they are recruited, are unable to properly organize them into visible punctate pre-pore structures.

Electron Microscopy Reveals an Absence of NPCs

As a last test, field emission scanning electron microscopy (FESEM) was performed in order to view the complex-depleted nuclear envelopes directly. This technique is capable of giving high resolution three-dimensional views of the nuclear envelope (Allen et al., 1998). With FESEM, the surfaces of mock-depleted nuclei were observed to contain abundant NPCs (Figure 7A). In contrast, the Nup107-160 complex-depleted nuclei were devoid of NPCs (Figure 7B). We conclude that the Nup107-160

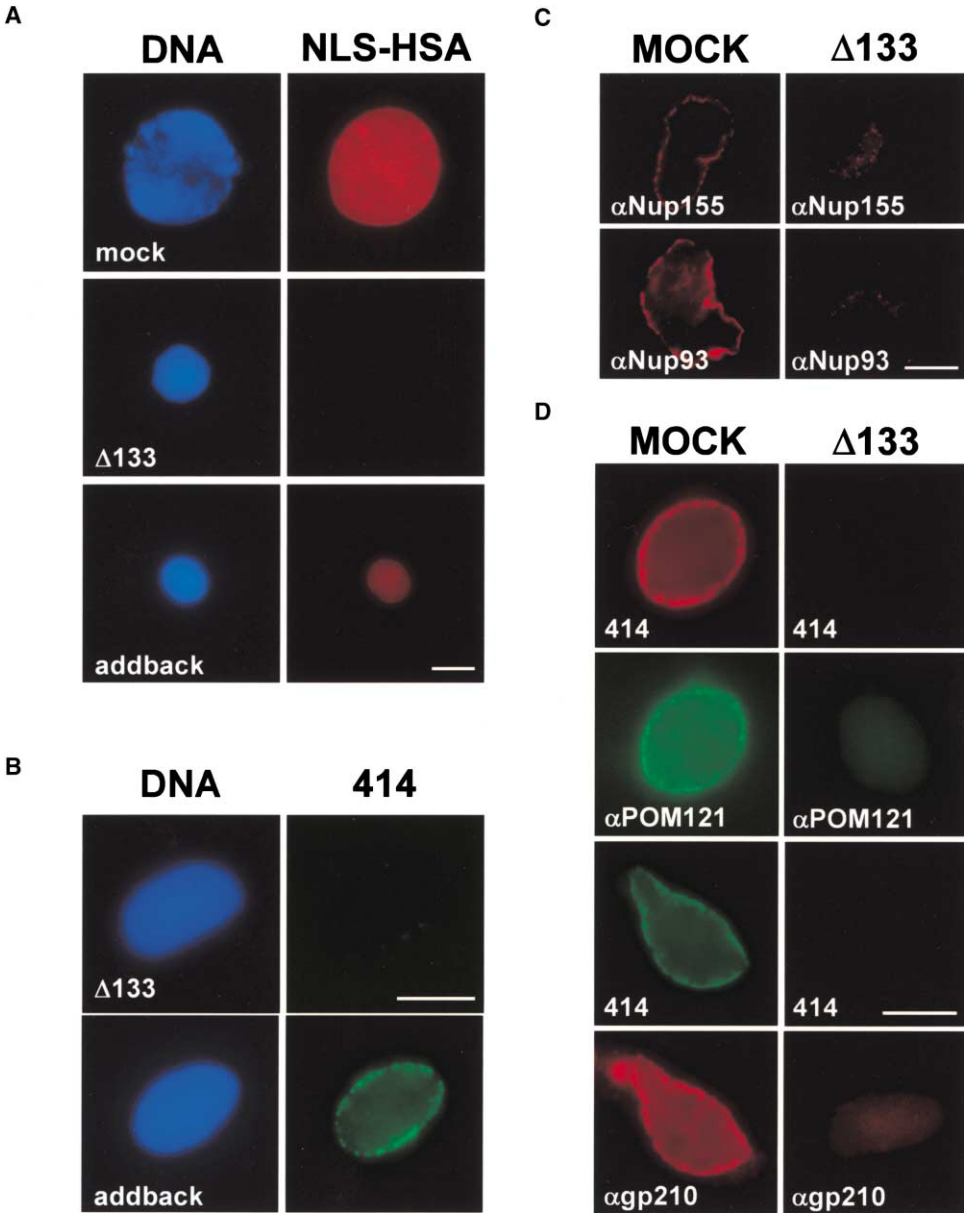

Figure 6. Nuclei Lacking the Nup107-160 Complex Are Defective for Multiple Nucleoporins Including the POM121 and gp210 Integral Membrane Nucleoporins

(A) Anti-Nup133-depleted nuclei are defective for import of TRITC-NLS–HSA (Δ133), but can be rescued by addback of dilute purified Nup107-160 complex (addback). TRITC-NLS-HSA was added 60 min after nuclear assembly was initiated and visualized 15 min later.

(B) Nuclei from an experiment similar to that in (A) were stained with Oregon green-labeled mAb414. No staining of mAb414 on the Δ133-depleted nuclei (Δ133) was observed. However, a bright punctate NPC stain was observed in Δ133-depleted nuclei to which purified Nup107-160 complex had been added at t = 0 (addback).

(C) Nuclei lacking the Nup107-160 complex were completely devoid of a nuclear rim stain for Nup155 and Nup93. Only a faint residual intranuclear stain was observed. For this, nuclei were assembled 60 min, fixed, and processed for indirect immunofluorescence.

(D) The NPC integral membrane proteins POM121 and gp210 appeared either absent or unorganized into punctate structures in nuclei lacking the Nup107-160 complex (Δ133). For this, mock- and Δ133-depleted nuclei were assembled 60 min, fixed, and then stained with TAMRA-labeled mAb414 and Oregon green-labeled anti-POM121 (top four panels), or Oregon green-labeled mAb414 and Texas red-labeled anti-gp210 (bottom four panels). With either anti-POM121 or anti-gp210 antibodies, only faint diffuse membrane stain was observed in Δ133-depleted nuclei, while with mAb414, fluorescence was absent altogether. The bars represent 10 μm.

complex-depleted nuclei are defective for the earliest visible steps in NPC assembly.

Discussion

In this study, we have identified an essential core element of the vertebrate nuclear pore, the Nup107-160 complex. Nuclei reconstituted in vitro lacking this complex contain nuclear membranes, but are small and virtually incapable of NLS import and DNA replication. Strikingly, these defects stem from the fact that the depleted nuclei are unable to assemble or maintain any nuclear pore complexes. This profound defect in pore assembly is clearly visible by FESEM microscopy. The full extent of

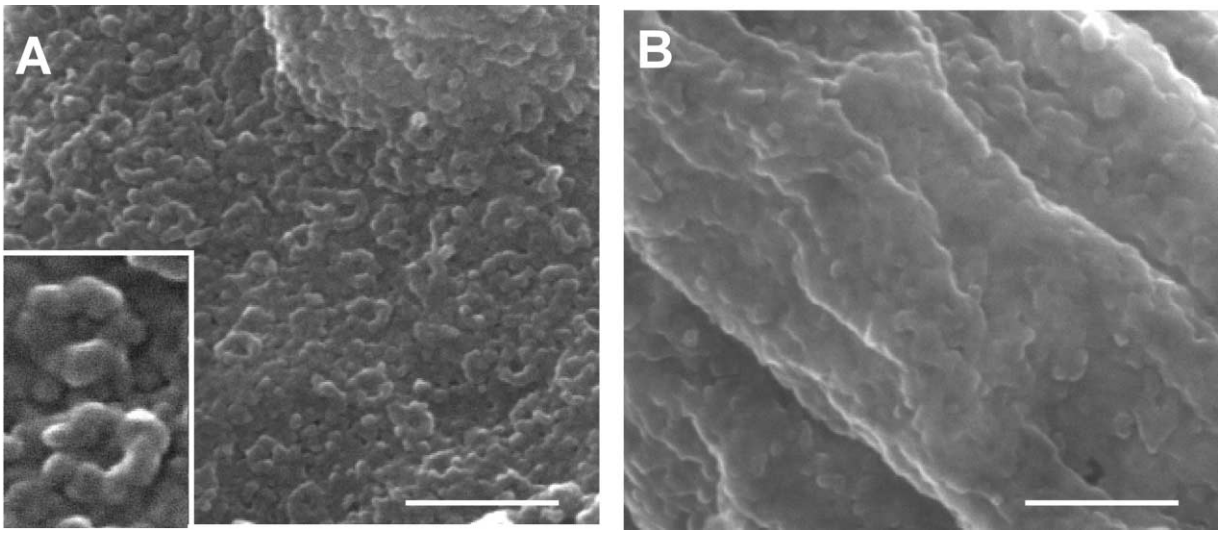

Figure 7. Nuclei Formed in the Absence of the Nup107-160 Complex Lack NPCs

Nuclei prepared from mock-depleted (A) and anti-Nup133 depleted (B) cytosol were examined with FESEM electron microscopy. Typical views are shown. Abundant NPCs with 8-fold symmetry can be seen in mock-depleted nuclei (A) but not in Δ133-depleted nuclei (B). The inset is at 3× higher magnification. The bars represent 500 nm.

the defect is apparent even at the level of the membrane proteins POM121 and gp210, which appear greatly diminished and unorganized in the nuclear membranes.

The use of two different antibodies for immunodepletion, anti-Nup85 and anti-Nup133, ties the specificity of the defect directly to the loss of the Nup107-160 complex. No other nucleoporins were depleted from the extract with the exception of a fraction of Nup98. Since complete immunodepletion of Nup98 gives rise to nuclei with intact NPCs capable of efficient import (Powers et al., 1997), Nup98 cannot be playing a role in the severe defects we observe here. Thus, we can attribute the defect in NPC assembly to the loss of the Nup107-160 complex itself. The observed restoration of NPC assembly and functional import after addback of the purified complex reinforces the conclusion that the Nup107-160 complex is a major determinant of NPC assembly.

Our identification of Nup85 in the vertebrate Nup107-160 complex raises interesting structural issues. In yeast, the analogous Nup84 complex is Y-shaped, with Nup85 and seh1 forming one arm of the Y (Siniossoglou et al., 2000). It has been suggested that multiples of the yeast Y may combine to form a structure akin to the eight-pointed "star ring" observed on the cytoplasmic face of *Xenopus* NPCs (Goldberg et al., 1997; Belgareh et al., 2001). With the identification of vertebrate Nup85, all the major components are now present to form a putative vertebrate Y-shaped complex. We think it likely that multiples of the Nup107-160 complex form a portion of the central scaffold of the vertebrate NPC.

High-resolution FESEM verified that NPCs are absent in Nup107-160 complex-depleted nuclei. It is still possible that an early NPC assembly intermediate forms, but is not visible with FESEM. If so, this putative NPC intermediate must not contain fluorescently measurable amounts of the soluble nucleoporins tested nor any highly organized POM121 or gp210 multimers. Since the membranes also stain significantly more faintly with POM121 and gp210 antibodies, there may be an additional defect in recruitment of the correct type of membrane vesicles to the chromatin. *Xenopus* egg extracts have been reported to contain two types of vesicles, one capable of ER-type membrane fusion, which initiates nuclear assembly, and a second capable of promoting NPC formation (Vigers and Lohka, 1991; Wiese et al., 1997; Drummond et al., 1999; Hetzer et al., 2001, and references therein). One speculative model would be that in the absence of the Nup107-160 complex the second class of vesicles may not be recruited efficiently to the chromatin.

The molecular mechanisms governing nuclear membrane assembly and its coordination with NPC assembly, despite being the focus of intense research, are poorly defined at present (Macaulay and Forbes, 1996; Zhang and Clark, 2000; Hetzer et al., 2001; Marelli et al., 2001; Ryan and Wente, 2002). Nuclear pore complex assembly is hypothesized to begin with the interaction of an integral membrane pore protein and a soluble protein. This interaction is hypothesized to cause multimerization of the membrane protein, which then leads to a fusogenic event that links the two nuclear membranes through a small fusion pore (10–30 Å) (Macaulay and Forbes, 1996; Goldberg et al., 1997). Over a hundred copies of cytoplasmic nucleoporin subcomplexes must then be recruited to the fusion pore to build the large NPC (1000 Å × 2000 Å). Almost no evidence exists to give molecular detail to this assembly model. Recently, gp210 antibodies and fragments were reported to block NPC assembly at a step following inner and outer nuclear membrane fusion and possibly also at an earlier step (Drummond and Wilson, 2002). Oddly, gp210 in HeLa cells arrives quite late in NPC assembly, after POM121 and many of the soluble nucleoporins have been incorporated (Bodoor et al., 1999). This does not rule out a possible transient role for gp210 in the fusion or post-fusion steps of assembly. It will be of interest to place the Nup107-160 complex, which arrives early to the NPCs of HeLa cells (Belgareh et al., 2001) and to the

chromatin in *Xenopus* reconstitution assays (R. Chan, A.V.O., and D.J.F., unpublished data), into this NPC assembly model.

In summary, we have found that reconstitution of nuclei lacking the Nup107-160 complex results in the most severe defect in NPC assembly yet observed, i.e., the full loss of the nuclear pore complex. We conclude that the Nup107-160 complex is an essential core element of the NPC and is used very early in the decision to form a nuclear pore. The Nup107-160 complex thus additionally offers an attractive point for regulation of nuclear pore complex assembly.

Experimental Procedures

cDNA Cloning and Antibody Production

A BLAST search with *S. cerevisiae* Nup85p (744 aa; gi 6322502) revealed a potential *S. pombe* homolog of 675 aa with 19% identity, but no vertebrate homologs. An iterative PSI-BLAST search, which uses the residues conserved between the two yeast Nup85s (Altschul et al., 1997), identified short mouse ESTs which could be combined to give a 656 aa ORF. A cDNA clone encoding this ORF was prepared by RT-PCR of mouse 3T3 total RNA and cloned into pET28a. His-tagged putative mouse Nup85 protein was expressed in *E. coli* BL21/DE3 and used for rabbit immunization. Relatives of mouse Nup85 (gi 12856972) were found, in many cases as the genomes were completed, in humans (656 aa; gi 10434102), *Drosophila* (668 aa; gi 7302655), *C. elegans* (598 aa; gi 17508241), *Arabidopsis thaliana* (713 aa; gi 18418112), rice (733 aa; gi 21902047), *Yarrowia lipolytica* (708 aa; gi 18076820), and *S. pombe* (675 aa; gi 19112685).

Antibodies were raised to recombinant human Nup133 containing all but seven C-terminal amino acids (aa 1–1149) (Vasu et al., 2001) and affinity purified as in Shah et al. (1998). Preimmune IgG from the same rabbits was purified with protein A-Sepharose. Immunoprecipitations were performed as in Shah et al. (1998) using affinity-purified IgG to mNup85 (aa 1–656), hNup133 (aa 1–1149), or preimmune antisera (1 μg) from the same rabbits. HeLa cells, grown in a 100 mm plate, were resuspended in 500 μl HMN buffer (20 mM *H*EPES [pH 7.5], 2.5 mM *M*gCl_2, and 150 mM *N*aCl), passed through a 22-gauge needle ten times, and incubated with ovalbumin-blocked antibody beads. Rat liver nuclei (12,000/μl) were prepared as in Finlay et al. (1991). Purified pores from *Xenopus* annulate lamellae (Miller and Forbes, 2000) were partially solubilized in 0.5 M NaCl, 0.5% Tween-20 in HM buffer (see above), diluted 10× in HMN, and immunoprecipitated.

Transfection, Immunofluorescence, and RNAi

HeLa cells on coverslips were transfected 16 hr with mouse Nup85 in a pCS2MT vector using Effectene (QIAGEN). The cells were methanol fixed (15 min −20°C), permeabilized (PBS/0.2% Triton X-100), blocked (10 min, PBS/0.2% Triton X-100/5% fetal calf serum), and incubated with anti-c-*myc* tag antibody (9E10; Calbiochem; 1 hr). Coverslips, mounted with Vectashield (Vector Laboratories), were visualized with a Zeiss Axioskop 2 microscope (63× objective). Immunofluorescence on interphase and mitotic HeLa cells was as in Vasu et al. (2001). For RNAi, HeLa cells were transfected for 3 days using 0.84 μg of Nup85 oligomer duplex (target: AACCCCTGGA CAACATCTTGTT) or control luciferase oligomer duplex (Xeragon; Huntsville, AL) in Oligofectamine (Invitrogen), followed by methanol fixation and immunofluorescence. DNA was stained with Hoechst 33258 or DAPI dye.

Antibodies

The antibodies used included affinity-purified anti-mouse Nup85 (aa 1–656); anti-human Nup133 (this study). Anti-human Nup160, anti-rat Nup98 (aa 43–470), and anti-rat Nup155 (aa 295–578) were described in Vasu et al. (2001). Also used were anti-Tpr (Shah et al., 1998); anti-hNup205 and anti-Nup93 (Miller and Forbes, 2000); anti-mouse Gle2 (a gift from M. Powers, Emory University, Atlanta, GA), mAb414 (Covance); anti-importin α, anti-importin β, and anti-transportin (Transduction Laboratories); anti-*Xenopus* POM121 (A.H. and D.J.F., unpublished data); anti-*Xenopus* Nup153 (Shah et al., 1998); anti-*Xenopus* Nup214 (Shah et al., 1998); anti-*Xenopus* gp210 lumenal domain (R. Chan and D.J.F., unpublished data); and anti-hsec13p antibody (see Vasu et al., 2001, for details). Indirect immunofluorescence and immunoblot analysis were done as in Shah et al. (1998).

Immunodepletion and Nuclear Reconstitution

Cytosolic and membrane vesicle fractions of *Xenopus* egg extracts were prepared as in Powers et al. (1995), except for the use of 500 mM KCl in the membrane wash buffer to remove residual amounts of soluble nucleoporins. The membranes were stored in 10 μl aliquots at −80°C, and used as a 20X stock. For immunodepletion, 300 μg of anti-Nup85, 600 μg of anti-Nup133 IgG, or equal amounts of preimmune IgG from the same rabbits were bound to 60 μl of protein A-Sepharose overnight. The bound antibody beads were blocked with 20 mg/ml BSA in PBS buffer and washed two to three times with ELB (Powers et al., 1995). Egg cytosol (200 μl) was added to 30 μl of antibody or preimmune IgG beads and tumbled 1 hr (4°C), giving a ratio of 1.5 (or 3.0 for Nup133) μg antibody/μl cytosol, for two consecutive depletions. The immuno- or mock-depleted cytosols were used for nuclear reconstitution by mixing with membrane vesicles and demembranated sperm chromatin (Powers et al., 1995). DNA replication was assayed as in Grandi et al. (1997). For indirect immunofluorescence, reconstituted nuclei were fixed, pelleted onto poly-lysine-coated coverslips (Macaulay and Forbes, 1996), and probed with various antibodies. For direct immunofluorescence, mAb414 or affinity-purified anti-POM121 or -gp210 antibodies were coupled to succinimidyl ester derivatives of Oregon green 488, Tetra-methyl-rhodamine (TAMRA), or Texas-redX (Molecular Probes, Eugene, OR). For this, nuclei were fixed with 3% formaldehyde, quenched with glycine, washed, and mixed with antibody. To assess nuclear import, TRITC-SV40 NLS-HSA transport substrate was added 60 min after the start of assembly and visualized 15–30 min later. For addback experiments, the Nup107-160 complex was purified by large-scale anti-Nup133 immunoprecipitation from *Xenopus* egg cytosol. For this, affinity-purified antibody was coupled to protein A-Sepharose, blocked with ovalbumin, and incubated in egg cytosol (2 ml) diluted in 50 ml PBS. The beads were washed extensively with PBS, once with 1 M NaCl, 50 mM Tris-HCl, and 1 mM DTT (pH 7.5), then eluted with 1 M $MgCl_2$, 1 mM DTT (pH 6.5). Purified complex was subjected to step dialysis into ELB minus sucrose and tested by adding 1/6 volume of highly purified complex (or buffer) to a Δ133 extract, followed by nuclear reconstitution and assessment of import and mAb414 staining.

Field Emission Scanning Electron Microscopy

Mock- and anti-Nup133 depleted nuclei were assembled for 60 min as above, then prepared essentially as in Allen et al. (1998). Samples were critical point dried from ultra-dry CO_2 (BAL-TEC CPD 030), sputter coated with 3.4 nm chromium (EMITECH K575X), and examined using a Philips XL30 ESEM FEG field emission scanning electron microscope.

Acknowledgments

The authors thank S. Allen for sequence searches, V. Delmar, M. Aviguetero, Zhongsheng You, and K. Wilson of U.C.S.D. for help with experimental techniques, and R. Chan for use of her gp210 antibody prior to publication. M.E. thanks Terry Allen for generous instruction in FESEM. This work was funded by a grant from the NIH (RO1 GM33279) to D.J.F., a United States-Israel Binational Science Foundation grant to M.E. and D.J.F., funding from the Marcus Sieff Foundation to M.E., and GANN Predoctoral Fellowships to A.V.O. and T.V.

Received: November 25, 2002
Revised: March 7, 2003
Accepted: March 13, 2003
Published: April 17, 2003

References

Aitchison, J.D., Blobel, G., and Rout, M.P. (1995). Nup120p: A yeast nucleoporin required for nuclear pore distribution and mRNA transport. J. Cell Biol. *131*, 1659–1675.

Allen, T.D., Rutherford, S.Z., Bennion, G.R., Wiese, C., Riepert, S., Kiseleva, E., and Goldberg, M.W. (1998). Three-dimensional surface structure analysis of the nucleus. In Methods in Cell Biology, Vol. 53, M. Berrios, ed. (San Diego: Academic Press), pp. 125–138.

Altschul, S.F., Madden, T.L., Schaffer, A.A., Zhang, J., Zhang, Z., Miller, W., and Lipman, D.J. (1997). Gapped BLAST and PSI-BLAST: a new generation of protein database search programs. Nucleic Acids Res. *25*, 3389–3402.

Bastos, R., Lin, A., Enarson, M., and Burke, B. (1996). Targeting and function in mRNA export of nuclear pore complex protein Nup153. J. Cell Biol. *134*, 1141–1156.

Belgareh, N., Rabut, G., Bai, S.W., van Overbeek, M., Beaudouin, J., Daigle, N., Zatsepina, O.V., Pasteau, F., Labas, V., Fromont-Racine, M., et al. (2001). An evolutionarily conserved nuclear pore subcomplex, which redistributes in part to kinetochores in mammalian cells. J. Cell Biol. *152*, 1147–1160.

Blow, J.J., and Laskey, R.A. (1986). Initiation of DNA replication in nuclei and purified DNA by a cell-free extract of Xenopus eggs. Cell *47*, 577–587.

Bodoor, K., Shaikh, S., Salina, D., Raharjo, W.H., Bastos, R., Lohka, M., and Burke, B. (1999). Sequential recruitment of NPC proteins to the nuclear periphery at the end of mitosis. J. Cell Sci. *112*, 2253–2264.

Boehmer, T., Enninga, J., Dales, S., Blobel, G., and Zhong, H. (2003). Depletion of a single nucleoporin, Nup107, prevents the assembly of a subset of nucleoporins into the nuclear pore complex. Proc. Natl. Acad. Sci. USA *100*, 981–985.

Conti, E., and Izaurralde, E. (2001). Nucleocytoplasmic transport enters the atomic age. Curr. Opin. Cell Biol. *13*, 310–319.

Cronshaw, J.M., Krutchinsky, A.N., Zhang, W., Chait, B.T., and Matunis, M.J. (2002). Proteomic analysis of the mammalian nuclear pore complex. J. Cell Biol. *158*, 915–927.

Cullen, B.R. (2001). Journey to the center of the cell. Cell *105*, 697–700.

Damelin, M., and Silver, P.A. (2000). Mapping interactions between nuclear transport factors in living cells reveals pathways through the nuclear pore complex. Mol. Cell *5*, 133–140.

Dimaano, C., Bal, J.R., Prunuske, A.J., and Ullman, K.S. (2001). RNA association defines a functionally conserved domain in the nuclear protein Nup153. J. Biol. Chem. *276*, 45349–45357.

Doye, V., Wepf, R., and Hurt, E.C. (1994). A novel nuclear pore protein Nup133p with distinct roles in poly(A)+ RNA transport and nuclear pore distribution. EMBO J. *13*, 6062–6075.

Drummond, S.P., and Wilson, K.L. (2002). Interference with the cytoplasmic tail of gp210 disrupts "close apposition" of nuclear membranes and blocks nuclear pore dilation. J. Cell Biol. *158*, 53–62.

Drummond, S., Ferrigno, P., Lyon, C., Murphy, J., Goldberg, M., Allen, T., Smythe, C., and Hutchison, C.J. (1999). Temporal differences in the appearance of NEP-B78 and an LBR-like protein during Xenopus nuclear envelope reassembly reflect the ordered recruitment of functionally discrete vesicle types. J. Cell Biol. *144*, 225–240.

Elbashir, S.M., Harborth, J., Lendeckel, W., Yalcin, A., Weber, K., and Tuschl, T. (2001). Duplexes of 21-nucleotide RNAs mediate RNA interference in cultured mammalian cells. Nature *411*, 494–498.

Feldherr, C.M., Akin, D., and Cohen, R.J. (2001). Regulation of functional nuclear pore size in fibroblasts. J. Cell Sci. *114*, 4621–4627.

Finlay, D.R., Meier, E., Bradley, P., Horecka, J., and Forbes, D.J. (1991). A complex of nuclear pore proteins required for pore function. J. Cell Biol. *114*, 169–183.

Fontoura, B.M., Blobel, G., and Matunis, M.J. (1999). A conserved biogenesis pathway for nucleoporins: proteolytic processing of a 186-kilodalton precursor generates Nup98 and the novel nucleoporin, Nup96. J. Cell Biol. *144*, 1097–1112.

Forbes, D.J., Kirschner, M.W., and Newport, J.W. (1983). Spontaneous formation of nucleus-like structures around bacteriophage DNA microinjected into Xenopus eggs. Cell *34*, 13–23.

Goldberg, M.W., Wiese, C., Allen, T.D., and Wilson, K.L. (1997). Dimples, pores, star-rings, and thin rings on growing nuclear envelopes: evidence for structural intermediates in nuclear pore complex assembly. J. Cell Sci. *110*, 409–420.

Goldstein, A.L., Snay, C.A., Heath, C.V., and Cole, C.N. (1996). Pleiotropic nuclear defects associated with a conditional allele of the novel nucleoporin Rat9p/Nup85p. Mol. Biol. Cell *7*, 917–934.

Gorlich, D., and Kutay, U. (1999). Transport between the cell nucleus and the cytoplasm. Annu. Rev. Cell Dev. Biol. *15*, 607–660.

Grandi, P., Dang, T., Pane, N., Shevchenko, A., Mann, M., Forbes, D., and Hurt, E. (1997). Nup93, a vertebrate homologue of yeast Nic96p, forms a complex with a novel 205-kDa protein and is required for correct nuclear pore assembly. Mol. Biol. Cell *8*, 2017–2038.

Greber, U.F., Senior, A., and Gerace, L. (1990). A major glycoprotein of the nuclear pore complex is a membrane-spanning polypeptide with a large lumenal domain and a small cytoplasmic tail. EMBO J. *9*, 1495–1502.

Griffis, E.R., Altan, N., Lippincott-Schwartz, J., and Powers, M.A. (2002). Nup98 is a mobile nucleoporin with transcription-dependent dynamics. Mol. Biol. Cell *13*, 1282–1297.

Hallberg, E., Wozniak, R.W., and Blobel, G. (1993). An integral membrane protein of the pore membrane domain of the nuclear envelope contains a nucleoporin-like region. J. Cell Biol. *122*, 513–521.

Hetzer, M., Meyer, H.H., Walther, T.C., Bilbao-Cortes, D., Warren, G., and Mattaj, I.W. (2001). Distinct AAA-ATPase p97 complexes function in discrete steps of nuclear assembly. Nat. Cell Biol. *3*, 1086–1091.

Hinshaw, J.E., Carragher, B.O., and Milligan, R.A. (1992). Architecture and design of the nuclear pore complex. Cell *69*, 1133–1141.

Kalab, P., Weis, K., and Heald, R. (2002). Visualization of a Ran-GTP gradient in interphase and mitotic Xenopus egg extracts. Science *295*, 2452–2456.

Li, O., Heath, C.V., Amberg, D.C., Dockendorff, T.C., Copeland, C.S., Snyder, M., and Cole, C.N. (1995). Mutation or deletion of the *S. cerevisiae RAT3/NUP133* gene causes temperature-dependent nuclear accumulation of poly(A+) RNA and constitutive clustering of nuclear pore complexes. Mol. Biol. Cell *6*, 401–417.

Lohka, M.J., and Masui, Y. (1983). Formation in vitro of sperm pronuclei and mitotic chromosomes induced by amphibian ooplasmic components. Science *220*, 719–721.

Lutzmann, M., Kunze, R., Buerer, A., Aebi, U., and Hurt, E. (2002). Modular self-assembly of a Y-shaped multiprotein complex from seven nucleoporins. EMBO J. *21*, 387–397.

Lyman, S.K., and Gerace, L. (2001). Nuclear pore complexes: dynamics in unexpected places. J. Cell Biol. *154*, 17–20.

Macara, I.G. (2002). Why FRET about Ran? Dev. Cell *2*, 379–380.

Macaulay, C., and Forbes, D.J. (1996). Assembly of the nuclear pore: biochemically distinct steps revealed with NEM, GTPγS, and BAPTA. J. Cell Biol. *132*, 5–20.

Marelli, M., Lusk, C.P., Chan, H., Aitchison, J.D., and Wozniak, R.W. (2001). A link between the synthesis of nucleoporins and the biogenesis of the nuclear envelope. J. Cell Biol. *153*, 709–724.

Matsuoka, Y., Takagi, M., Ban, T., Miyazaki, M., Yamamoto, T., Kondo, Y., and Yoneda, Y. (1999). Identification and characterization of nuclear pore subcomplexes in mitotic extract of human somatic cells. Biochem. Biophys. Res. Commun. *254*, 417–423.

Miller, B.R., and Forbes, D.J. (2000). Purification of the vertebrate nuclear pore by biochemical criteria. Traffic *1*, 941–951.

Newport, J. (1987). Nuclear reconstitution in vitro: stages of assembly around protein-free DNA. Cell *48*, 205–217.

Powers, M.A., Macaulay, C., Masiarz, F.R., and Forbes, D.J. (1995). Reconstituted nuclei depleted of a vertebrate GLFG nuclear pore protein, p97 (Nup98), import but are defective in nuclear growth and replication. J. Cell Biol. *128*, 721–736.

Powers, M.A., Forbes, D.J., Dahlberg, J.E., and Lund, E. (1997). The vertebrate GLFG nucleoporin, Nup98, is an essential component of multiple RNA export pathways. J. Cell Biol. *136*, 241–250.

Reichelt, R., Holzenburg, A., Buhle, E.L., Jr., Jarnik, M., Engel, A., and Aebi, U. (1990). Correlation between structure and mass distri-

bution of the nuclear pore complex and of distinct pore complex components. J. Cell Biol. *110*, 883–894.

Ribbeck, K., and Gorlich, D. (2002). The permeability barrier of nuclear pore complexes appears to operate via hydrophobic exclusion. EMBO J. *21*, 2664–2671.

Rout, M.P., Aitchison, J.D., Suprapto, A., Hjertaas, K., Zhao, Y., and Chait, B.T. (2000). The yeast nuclear pore complex. Composition, architecture, and transport mechanism. J. Cell Biol. *148*, 635–652.

Ryan, K.J., and Wente, S.R. (2002). Isolation and characterization of new *Saccharomyces cerevisiae* mutants perturbed in nuclear pore complex assembly. BMC Genet. *3*, 17.

Sazer, S., and Dasso, M. (2000). The ran decathlon: multiple roles of Ran. J. Cell Sci. *113*, 1111–1118.

Schwoebel, E.D., Ho, T.H., and Moore, M.S. (2002). The mechanism of inhibition of Ran-dependent nuclear transport by cellular ATP depletion. J. Cell Biol. *157*, 963–974.

Shah, S., Tugendreich, S., and Forbes, D. (1998). Major binding sites for the nuclear import receptor are the internal nucleoporin Nup153 and the adjacent nuclear filament protein Tpr. J. Cell Biol. *141*, 31–49.

Shamsher, M.K., Ploski, J., and Radu, A. (2002). Karyopherin beta 2B participates in mRNA export from the nucleus. Proc. Natl. Acad. Sci. USA *99*, 14195–14199.

Shaywitz, D.A., Orci, L., Ravazzola, M., Swaroop, A., and Kaiser, C.A. (1995). Human SEC13Rp functions in yeast and is located on transport vesicles budding from the endoplasmic reticulum. J. Cell Biol. *128*, 769–777.

Siebrasse, J.P., and Peters, R. (2002). Rapid translocation of NTF2 through the nuclear pore of isolated nuclei and nuclear envelopes. EMBO Rep. *3*, 887–892.

Siniossoglou, S., Wimmer, C., Rieger, M., Doye, V., Tekotte, H., Weise, C., Emig, S., Segref, A., and Hurt, E.C. (1996). A novel complex of nucleoporins, which includes sec13p and a sec13p homologue, is essential for normal nuclear pores. Cell *84*, 265–275.

Siniossoglou, S., Lutzmann, M., Santos-Rosa, H., Leonard, K., Mueller, S., Aebi, U., and Hurt, E. (2000). Structure and assembly of the Nup84p complex. J. Cell Biol. *149*, 41–54.

Ullman, K.S., and Forbes, D.J. (1995). RNA polymerase III transcription in synthetic nuclei assembled in vitro from defined DNA templates. Mol. Cell. Biol. *15*, 4873–4883.

Ullman, K., Shah, S., Powers, M., and Forbes, D. (1999). The nucleoporin Nup153 plays a critical role in multiple types of nuclear export. Mol. Biol. Cell *10*, 649–664.

Vasu, S., and Forbes, D.J. (2001). Nuclear pores and nuclear assembly. Curr. Opin. Cell Biol. *13*, 363–375.

Vasu, S., Shah, S., Orjalo, A., Park, M., Fischer, W.H., and Forbes, D.J. (2001). Novel vertebrate nucleoporins Nup133 and Nup160 play a role in mRNA export. J. Cell Biol. *155*, 339–354.

Vigers, G.P., and Lohka, M.J. (1991). A distinct vesicle population targets membranes and pore complexes to the nuclear envelope in Xenopus eggs. J. Cell Biol. *112*, 545–556.

Walther, T.C., Fornerod, M., Pickersgill, H., Goldberg, M., Allen, T.D., and Mattaj, I.W. (2001). The nucleoporin Nup153 is required for nuclear pore basket formation, nuclear pore complex anchoring and import of a subset of nuclear proteins. EMBO J. *20*, 5703–5714.

Walther, T.C., Pickersgill, H.S., Cordes, V.C., Goldberg, M.W., Allen, T.D., Mattaj, I.W., and Fornerod, M. (2002). The cytoplasmic filaments of the nuclear pore complex are dispensable for selective nuclear protein import. J. Cell Biol. *158*, 63–77.

Weis, K. (2002). Nucleocytoplasmic transport: cargo trafficking across the border. Curr. Opin. Cell Biol. *14*, 328–335.

Wiese, C., Goldberg, M.W., Allen, T.D., and Wilson, K.L. (1997). Nuclear envelope assembly in Xenopus extracts visualized by scanning EM reveals a transport-dependent 'envelope smoothing' event. J. Cell Sci. *110*, 1489–1502.

Yang, Q., Rout, M.P., and Akey, C.W. (1998). Three-dimensional architecture of the isolated yeast nuclear pore complex: functional and evolutionary implications. Mol. Cell *1*, 223–234.

Zhang, C., and Clarke, P.R. (2000). Chromatin-independent nuclear envelope assembly induced by Ran GTPase in Xenopus egg extracts. Science *288*, 1429–1432.